

ARTICLE

UV photobleaching of carbon nanodots investigated by in-situ optical methods

Received 00th January 20xx,
Accepted 00th January 20xx

DOI: 10.1039/x0xx00000x

A. V. Longo^{a,†}, A. Sciortino^a, M. Cannas^a, F. Messina^{a,*}

Carbon dots are a family of optically-active nanoparticles displaying a combination of useful properties that make them attractive for many applications in photonics and photochemistry. Despite initial claims of high photostability of carbon dots even under prolonged illuminations, several recent works have evidenced their photobleaching (PB) under UV light, detrimental for some applications. The mechanism and dynamics of carbon dot PB provides a useful route to gather relevant information on the underlying photophysics of these nanoparticles, still very debated. Here we report a study of the PB of carbon dots under UV light, conducted through a combination of in-situ optical experiments in well-controlled illumination conditions. Our experiments allow capturing the precise kinetics of the undergoing PB process, which is found to be significantly affected by disorder and photoselection effects. Furthermore, our study discloses several pieces of information on the nature of the main blue chromophore absorbing at 340 nm and emitting at 430 nm, and on its PB mechanism. We propose that the emissive units consist in small molecular-like chromophores adsorbed on carbon dot surfaces and living in a dynamical equilibrium with free diffusing molecules in solution. Their photobleaching proceeds in two distinct steps: in a first phase, linear absorption of UV photons rapidly converts the molecular surface chromophores into a non-emissive form, likely through an isomerization, causing the disappearance of the fluorescence properties but almost no changes in the optical absorption spectra. At higher fluences, a complete destruction of the optically-active centers is observed, which completely wipes out all the absorption features of surface chromophores and only leaves a fully carbonized, yet non-fluorescent, dot core.

Introduction

The accidental discovery in 2004 of a new class of carbon-based nanomaterials [1], known nowadays as carbon dots (CDs), paved the way towards the study of a family of photoactive materials that is today still under continuous development [2, 3]. Indeed, these nanoparticles (NPs), usually structured as a spherical-shaped carbon core surrounded by a shell of chemical functional groups [4-5], own several characteristics that make them extremely attractive, for example a bright and tunable fluorescence and a high water dispersibility. In addition, CDs are believed to be highly biocompatible [6], in contrast to most common types of Quantum Dots, which can be considered their metal-based counterpart. It is possible to obtain CDs through a wide variety of techniques, either with a bottom-up or top-down approach,

resulting in a large range of structural characteristics and fluorescence properties [2, 3, 7-11]. Although the optical properties of CDs have already been successfully exploited in several applications, including bio-imaging [6, 12], photocatalysis [13], sensing [14-16], optoelectronics [17], there are still some critical points that need to be addressed in a more systematic way, such as thoroughly explaining the origin of the emission, the consequences of morphological and structural inhomogeneity, and the role of fluorescent molecular impurities. The latter, in particular, are the subject of a lively debate: being found as a common side product of bottom-up CD synthesis, they seem to have a remarkable effect on their optical properties, [18-23] largely neglected by the earliest studies.

The study of the PB process affecting CDs under prolonged or high intensity illumination can be considered as an useful route to characterize their photochemical response while fundamentally addressing the absorption and emission mechanisms. The term photobleaching (PB) is used to refer to the loss of the luminescence properties of a system exposed for a long time to the excitation source, especially in the UV region. In a broader sense, it can refer to the progressive disappearance of all the optical signatures of the system. CDs were initially described in the literature as insensitive to prolonged irradiation [4 24-27], which has been emphasized as

^aDipartimento di Fisica e Chimica "Emilio Segrè", Università degli Studi di Palermo, Via Archirafi 36, Palermo (Italy)

[†]Current Address : Université de Paris, ITODYS, CNRS, UMR 7086, 15 rue J-A de Baif, 75013 Paris, France

* fabrizio.messina@unipa.it

Electronic Supplementary Information (ESI) available: [details of any supplementary information available should be included here]. See DOI: 10.1039/x0xx00000x

a strong benefit with respect to organic fluorophores [28-31]. However, several later papers showed that, not only it is possible to observe a marked PB effect [32-37] for CDs, having a potentially detrimental effect in applications, but PB can interestingly be used as an efficient way to investigate CD properties. Like several other properties, also the PB response of CDs is very strongly dependent on the synthesis route and precise structure. For example, more than a paper reports that the nature of the carbon core (amorphous or crystalline) plays a role to determine the PB resistance of CDs, with the amorphous-core CDs being more sensible to the effect of UV irradiation [35, 37, 38]. Besides, one may expect that any fluorescent organic dyes produced in the synthesis, attached or not to CD surfaces, should be particularly prone to PB effects. In this context, several papers tried to explore routes to improve the photostability of CDs through a suitable tailoring of their structures. For example, Wang et al [34] showed that increasing both the temperature or the reaction time of the hydrothermal treatment of citric acid and Urea in order to obtain nitrogen-doped CDs, improves the PB resistance of the CDs obtained, and suggested that this behavior results from an increased carbonization of the surface molecular structures responsible of the fluorescence. Analogous studies were carried on by He et al. [33] and Xiong et al. [39], who also explored how CDs produced by different precursors differ in term of their response to PB effects. Anyway, the question of fully understanding and controlling PB effect remains largely open, despite its importance in applications.

In this work, we introduce an original technique to study the PB phenomenon, founded on an *in situ* analysis of the process, almost unprecedented in literature [34], through the implementation of an experimental setup built ad hoc for this purpose. This new approach entails several advantages compared to the previous studies: first, it allows to determine the exact kinetic of the undergoing PB process, which was not revealed by previous studies, and consequently discloses several additional information difficult to capture with traditional *ex-situ* methods. Moreover, while previous studies typically used a simple UV lamp to induce photobleaching [33-35, 38], here we used a pulsed laser as irradiation source. In this way, we are able to rigorously control and test the role of some relevant parameters, such as the geometry of irradiation, spatially uniform or not, and the power received by the sample. The results reveal a variety of details on the mechanism and kinetics of carbon dot photobleaching. In particular, we propose that low-fluence UV irradiation initially causes a rapid PB through the isomerization of molecular-type fluorescent chromophores adsorbed on CD surfaces into a non-emissive form. This process is followed, at very high fluences, by the complete destruction of these chromophores, which finally leaves a non-emissive graphitic core.

Materials and methods

Synthesis of the CD Sample: The sample was prepared through a synthesis route already described in previous papers [40]. In short, CDs are obtained by microwave-induced

decomposition of an aqueous solution (10 ml) of citric acid (3 g) and urea (0.39 g) in a standard household microwave oven, using a nominal power of 600 W. The quantities of precursors chosen imply a nominal atomic ratio between nitrogen (N) and carbon (C) of 0.14. Under these conditions, the CDs obtained are characterized by a N-doped graphitic nanocrystalline core structure[40].

Steady-State Absorption: Optical spectra of CD solutions were recorded at room temperature in 1 cm quartz cuvettes with a double beam spectrophotometer (JASCO V-560) operating in the 250–900 nm range.

Steady-State Photoluminescence (PL): *ex-situ* PL spectra and two-dimensional (2D) excitation-emission maps were recorded at room temperature in 1 cm quartz cuvettes on a JASCO FP6500 spectrofluorometer equipped with a 150 W xenon lamp as a source, and a photomultiplier as detector, operating in the range 300–700 nm.

Time Resolved emission: Excited-state decay kinetics were measured using an Oportek Vibrant pulsed laser (5 ns pulsewidth), tunable in the range 210–2400 nm, as the excitation source, a Spectra Pro2300i PI Acton monochromator as dispersion stage, and a PI-MAX intensified CCD camera as acquisition device, which can be electronically gated in such a way to acquire the fluorescence intensity as a function of time delay after excitation. Thereby, lifetime values were obtained by least-square fitting of the time-dependent fluorescent intensities collected at the fluorescence emission peak. The time resolution of the lifetime measurement is determined by the laser pulsewidth, and is about 3 nanoseconds.

Photobleaching (PB) experiments: In order to induce a PB of the optical bands of CDs, the third (3.49 eV/355 nm) or fourth harmonic (4.66 eV/266 nm) of a Q-switched Nd:YAG Laser were used as a high-power light source (1–20 mJ per pulse, 5 ns pulse duration, 1 Hz) to irradiate the samples. As described in more detail in the results section, the optical properties of CDs dissolved in water were recorded before and after different irradiation treatments, in which the samples received variable numbers of high energy pulses from the Nd:YAG laser, directed to the sample in various optical geometries.

In-situ optical measurements: In some of the PB experiments, we carried out *in situ* optical absorption and PL measurements, in order to monitor in real-time the changes of the optical spectra of the samples induced by the progress of photobleaching. *In-situ* absorption spectra were collected by a single beam optic fiber spectrophotometer (Avantes S2000), while *in situ* PL measurements were carried out with the same equipment used for lifetime measurements. For these measurements, the intensified CCD camera was operated in such a way to acquire a time-integrated spectrum (equivalent to a steady-state emission measurement) after each excitation pulse. The full setup and procedures used in these experiments are further described in the results section.

Results and discussion

An overview of the optical properties of the CD sample object of this study, before any PB experiment, is shown in Figure 1, and it is well-representative of archetypal N-doped CDs as reported in many literature works [33, 41]. Their absorption spectrum (Figure 1a) is characterized by a sharp band peaking at 3.67 eV (338 nm), accompanied by a shoulder at lower energies, both of which sit over an unstructured absorption tail growing with increasing energy. From the 2D excitation-emission plot (Figure 1b), it can be inferred that the optical transition related to the main absorption band is responsible for most of the observed PL. A representative steady-state emission spectrum is shown in Figure 1a, recorded using an excitation energy of 3.54 eV (350 nm), which is the peak of the PL excitation spectrum (see Figure 1b). In these conditions, the emission maximum is found at 2.87 eV (432 nm) and displays a 0.55 eV full width at half maximum (FWHM). From Figure 1b it is possible to note that the emission displays some degree, although limited, of tunability (excitation wavelength-dependence), as the emission shifts toward a redder spectral range when excited at lower energies. Indeed, fluorescence tunability is well-known as a typical optical behaviour of CDs [4].

As an initial test for any PB effects, an aqueous CD solution was exposed to prolonged high-intensity irradiation by the third harmonic (3.49 eV/355 nm) of a Nd:YAG laser: 18000 pulses at a repetition rate of 1 Hz with 10 mJ energy/pulse. In these conditions, a strong PB effect is observed on both absorption and emission signals: as can be seen from Figure 1a, although the unstructured absorption tail remains unaltered, laser irradiation induces a remarkable reduction of the absorption bands intensity, accompanied by a quenching of the emission of a factor > 10.

In order to gain a comprehensive view of this PB process, activated by the high-intensity UV laser, we used *in situ* methods to monitor the progress of PB, using either PL or OA measurements as a probe. The experimental configurations used for these tests are described in detail in Figure 2. As sketched in Figure 2c, the in-situ PL experiments are performed using two different lasers in a pump/probe configuration. A low-power probe laser (350 nm/3.54 eV) is used to excite the fluorescence and measure its intensity variations induced by the exposure to the high-power UV laser, hereafter referred to as the PB laser. The probe laser, directed collinearly to the PB laser (see Figure 2c), was operated with much lower intensity (40 μ J/pulse) than the pump laser, and was synchronized in such a way to excite the sample during the interpulse time (fixed at 1 s) between successive PB pulses. Therefore, it was possible to acquire one fluorescence spectrum after each PB pulse. Similarly, to carry out in-situ optical absorption experiments, we used an optical fiber spectrophotometer (Figures 2a and 2b) capable of acquiring the full absorption spectrum (3.0 - 4.5 eV) of the sample within a few ms integration time. As seen in Figures 2a and 2b, the OA probe beam, produced by a lamp, is always perpendicular to the PB beam, but we used two different experimental geometries characterized by a uniform (panel b) or non-uniform (panel a) irradiation of the sample volume by the high-intensity PB beam. In both cases, the equipment was triggered to acquire an absorption spectrum after each PB pulse received by the sample. Therefore, by either of the two methods it was possible to monitor in real-time the evolution of the optical spectra during the course of irradiation and, therefore, of the PB. We checked that neither the probe laser nor the lamp used for the two types of in-situ experiments are capable, in themselves, to produce appreciable PB effects, at least at the fluences used in our measurements.

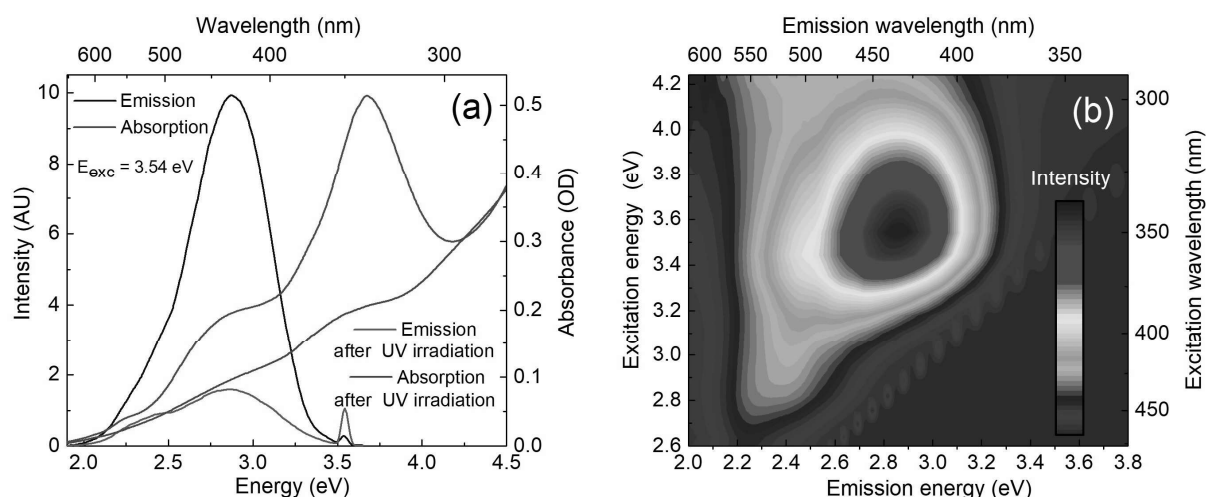


Figure 1: (a) Absorption and fluorescence spectra excited at 3.54 eV (blue line) of a 50 mg/L aqueous solution of CDs in a 1 cm square-base cuvette, before and after prolonged exposure to high intensity 3.49 eV laser irradiation. (b) 2D excitation-emission fluorescence intensity of water solution of as-synthesized CDs. The series of spots regularly arranged along a line is due to the revelation of the excitation radiation scattered by the sample.

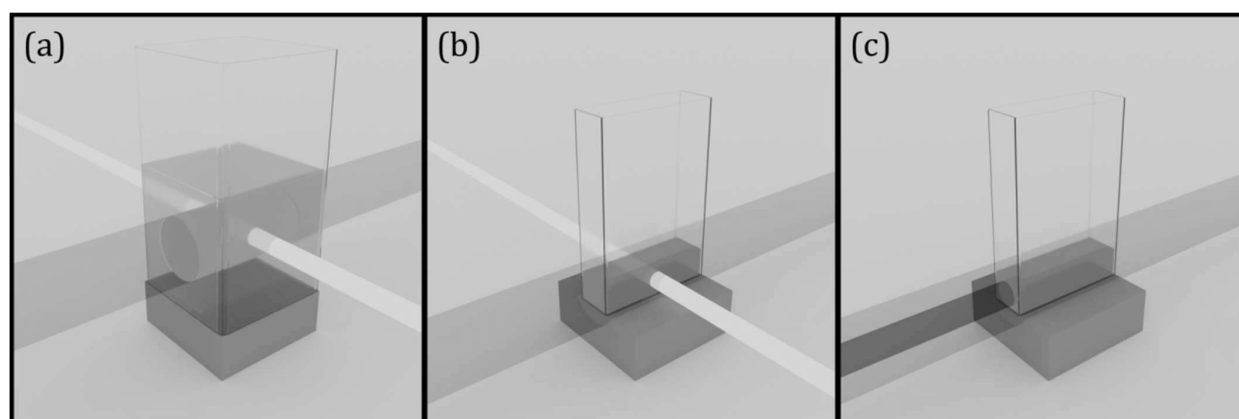


Figure 2: Geometrical arrangements used to carry out the in-situ PB experiments described in the text (a) In-situ OA measurements during a PB experiment in a non-uniform geometry. The PB laser (violet) irradiates a cylindrical volume within the sample, while a probe beam (yellow) transmitted by an optical fiber (not shown) is used to probe the OA spectrum of the sample (b) Same as panel (a), but in a uniform geometry. In this case, the experiment is carried out in a thinner cuvette, in such a way that the whole volume of the solution is illuminated by the PB laser. (c) In situ PL experiment, carried out in the uniform geometry. During irradiation by the PB laser, second, low-intensity laser (darker violet) is used to probe the emitted PL. Fluorescence is detected at 90° angle (not shown) relative to the excitation beam.

We first discuss the behaviour we observe when the PB experiment is conducted in deliberately non-uniform conditions, which we achieve as in Figure 2a. In this kind of PB experiment, we prepared a sample in a standard concentration of 50 mg/L, into a 1 cm square-base cuvette filled up to 3 cm height. Then, we exposed this sample to the PB beam, with intensity of 10 mJ/pulse and a repetition rate of 1 Hz, and used the optical fiber spectrophotometer to monitor the changes of the absorption spectrum. Under these conditions, considering that the beam diameter of the pump laser is $d_L \approx 5$ mm, not all the solution is irradiated by UV light, but the cylinder of irradiated sample is surrounded from all sides by non-exposed solution (see Figure 2a). In this condition we estimate that 10% or less of the sample volume is exposed to the PB beam. When conducting the experiment in this geometry, we found that if the irradiation is interrupted after few seconds, an almost total and stable recovery of the optical properties can be observed, as shown in Figure 3. More specifically, during the first 25 seconds of irradiation, the absorption of the sample is steeply reduced by photobleaching, but after the recovery process, whose duration is of the order of a few hundred seconds, >70% of the initial loss is recovered (Figure 3). This phenomenon is in all likelihood due to a diffusion effect exchanging chromophores between the cylindrical photobleached region of the cuvette and the unexposed part, a process usually referred to as a recovery after photobleaching [31]. In fact, the vast majority of the optically-active chromophores present in the solution initially reside

outside the photobleached region, and therefore are not affected by the pump laser during the irradiation phase. Therefore, during and after the end of irradiation they re-enter the experimental volume by diffusion, leading to the observed recovery of the absorption intensity. Our estimate of 70% recovery is almost certainly an underestimation, considering that the recovery is expected to begin immediately (that is, already during the 25 s duration of the irradiation), therefore leading to a reduction of the observed initial loss. Indeed, the data in Figure 3 are consistent with an almost total recovery, which, probably, is not complete only because the molecules initially outside the irradiated volume get slightly diluted over a larger volume when they come back into it. Obviously, our interpretation relies on the emissive chromophores being mobile enough to diffuse back in the irradiated volume within a time scale of a few hundreds of seconds. A rough estimate based on Einstein's equation $x^2 = 2Dt$, used over the time scale t of the recovery, with x of the order of the lateral size of the laser beam, implies a diffusion coefficient of the order of $10^{-5} \text{ cm}^2/\text{s}$. This order of magnitude is too small to be compatible with the size of the CDs studied (diameter of 3-4 nm). Indeed, considering that the experiment has been carried on at room temperature and in water, the Einstein Stokes-equation ($D = kT/6\pi\eta r$) relates such a value of D to a diffusing object as small as ≈ 0.5 nm. This is almost one order of magnitude smaller than the typical size of a CDs, and suggests that the object undergoing diffusion is a small molecular unit of the size of a single aromatic ring.

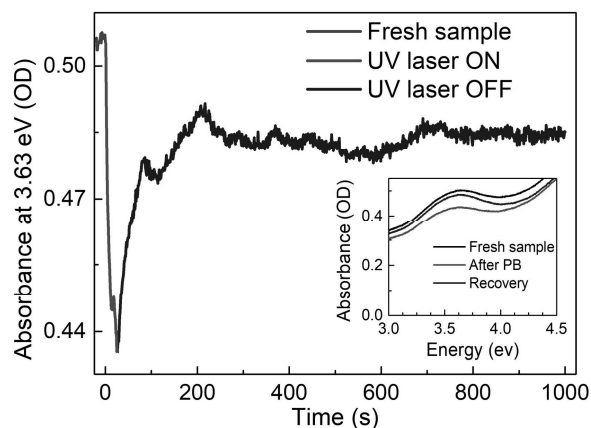


Figure 3: Kinetics of the absorption value at 3.63 eV which shows the decrease of the absorption due to the UV irradiation and the following recovery of the absorbance within a few hundred seconds after the UV irradiation is stopped. Inset: Absorption spectra of the fresh sample (black curve), of the sample immediately after irradiation (red curve) and after the recovery period (blue curve).

Therefore, these in situ experiments provide clear evidence of the role of small molecular chromophores in the observed fluorescence of CD samples, which was proposed by several works in the recent literature, although on very different grounds [19, 39, 42]. The present data demonstrate that at least a portion of the blue emission of these CDs can be attributed to sub-nm sized molecules freely diffusing in solution. In particular, considering the conditions in which our synthesis was carried out (microwave-induced decomposition of citric acid and urea), the existing literature suggests the free chromophore to be citrazinic acid [19, 20, 34, 39, 42-46], which is indeed characterized by a near-UV emission band in the same spectral region as found here [42]. As a matter of fact, the absorbance recovery shown in the inset of Figure 3 is mainly limited to the band at 3.7 eV attributed to citrazinic acid [19, 34, 47], whereas the higher-energy unstructured tail [48], due to the plasmonic absorption of the carbon cores [48], is not affected by the reported phenomenon.

With the aim of studying the detailed kinetics of the PB processes, we continued our experiments in a different geometry, allowing now to eliminate any effects of non-

uniformity. This experimental configuration is described in Figures 2b and 2c. During a typical experiment, we prepared a sample in a standard concentration of 50 mg/L, but this time the sample was put into a 1 x 0.1 mm cuvette (for *in-situ* PL measurements) or in a 1 x 0.5 cm cuvette (absorption measurements), filled only for a few mm height. Then, we exposed this sample to the high intensity laser beam, which crosses the sample through the shortest side of the cuvette. Under these conditions, the solution volume is small enough to be uniformly irradiated by UV light, because the beam diameter is larger than the height of the sample within the cuvette. Therefore, we expect this configuration should allow to avoid any kind of interfering phenomena like the one showed in Figure 3. In Figure 4 we report typical PL (panels a and b) and absorption (panels c and d) spectra recorded in situ during irradiation in uniform geometry. The power of the pump laser was fixed to 5 mJ/pulse and the repetition rate to 1 Hz, and the measurements were acquired at a rate of one PL or absorption spectrum per second. Figure 4a shows a selection of spectra obtained by in-situ PL: the luminescence intensity is progressively reduced with the increase of the number of pulses received by the sample. For instance, after 40 pulses the emission intensity is reduced to half of the initial value, and after 500 pulses only a value corresponding to the 10 % of the initial one is recorded. Through this method, it is possible to study the kinetics of the PB process in real time and full detail: Figure 4b displays the PB kinetics obtained by extracting the intensity value at the emission peak from every acquired spectrum. Interestingly, we found that the photobleaching kinetics cannot be reproduced by a standard exponential function. Instead, we needed to use a stretched exponential function $y(N) = e^{-\left(\frac{N}{N_0}\right)^\beta}$ to fit the data, where N is the number of pulses and N_0 is a fitting parameter. The stretched exponential decay suggests the presence of an inhomogeneity inside the sample, in terms of "switching off" probability, meaning that this probability is not the same for all the chromophores, but is distributed around the value N_0 . As in a standard exponential decay, the N_0 parameter is linked to the mean pulse number (or time) needed to bleach the sample. The value of β , always smaller than 1, is directly connected to the width of the distribution. The resulting fitting parameters are $N_0 = 48 \pm 5$ and $\beta = 0.60 \pm 0.05$. The low value of β , well below unity, indicates a very broad distribution inside the sample.

to many other organic dyes [28, 29, 31]. However, the data in Figure 4b provide a strong suggestion that the photophysics of our sample cannot entirely be ascribed to such small free molecules. In fact, a stretched exponential PB kinetics as in Figure 4b represents the typical behaviour of structurally disordered systems, thereby it suggests an active role of carbon dots in influencing the optical properties of the blue-emitting chromophore. Another clear evidence in this direction is the excited-state decay kinetics we record for the blue fluorescence (Figure S1b), which equally behaves as a stretched exponential: as a matter of fact, both the PB kinetics and the excited-state decay of a simple molecular dye in solution should rather be simple exponentials. Therefore, our data highlight an influence of CDs structural disorder on the emission, which is inconsistent with the simple picture of a solution of free photoluminescent molecules. This conclusion is further confirmed by the tunability of CD fluorescence (Figure 1b), another well-known consequence of dot-to-dot inhomogeneity [49]. These considerations suggest that the most probable scenario is a dynamical equilibrium between free molecules, and molecules temporarily bound to the disordered surface of CDs. In other words, the surface chromophore of these CDs seems to consist in a small molecular unit weakly attached to the surface, which participates to a dynamical equilibrium with a freely diffusing version of the same molecule. After photobleaching in a non-uniform geometry, it is thanks to this dynamical equilibrium that both species, and not only the free molecules, can be restored by back-diffusion from the non-irradiated volume. An interesting observation here is the absence of any clear single-exponential component in the decay and PB kinetics: their stretched-exponential nature, in contrast, suggests very broad distributions of decay and PB rates. This evidence suggests that, at any given time, most of the molecular chromophores are actually attached to CD surfaces, probably in different geometrical configurations, and the free diffusing molecules are a minority. However, the precise ratio between these two populations in thermodynamic equilibrium cannot be extracted from these data. Anyway, recalling (Figure 1) that a sufficiently prolonged irradiation completely wipes out any optical activity, there is no substantial difference between the photobleaching probability of the two forms (attached or not) of the fluorophores, both of which are easily destroyed by UV irradiation. Interestingly, after the end of the photobleaching process, the weak, residual fluorescence in the sample displays slightly different optical characteristics as compared to the native emission. In fact (Figure S1a), normalized spectra before and after PB demonstrate a slight shift and broadening of the emission band, while lifetime data collected before and after irradiation (Figure S1b) similarly demonstrate a slight change of the lifetime. Both these results are a sign of photo-selection

within an inhomogeneously broadened distribution of slightly different chromophores, due to their interaction with the surface of structurally different CDs.

After studying the PB kinetics with in-situ photoluminescence, we repeated the same experiment carried out in spatially uniform conditions but, this time, instead of using the PL as a probe, we used in-situ optical absorption to monitor the variations of the sample during the irradiation process (Figure 2b). On one hand, it is evident that the photobleaching affects not only the fluorescence intensity, but also the intensity of the main absorption band of the sample, which strongly decreases with increasing number of PB pulses. Notably, we found no recovery effect if the irradiation is interrupted, which confirms our previous interpretation of Figure 3 as an effect of diffusion. Besides, while the main absorption band is cancelled by PB (Figure 4c), the underlying, unstructured absorption tail is not affected, which suggests that PB only affects the surface chromophores, and the free molecules in equilibrium with them, but not the core structure of the CD. In fact, the unstructured absorption tail should be essentially related to the π plasmonic absorption of graphitic CD cores [48]. However, the most interesting observation comes from comparing the two types of in situ kinetics. The kinetics of the absorption coefficient at the peak, shown in Figure 4d, is markedly different from that of the fluorescence: after about 100 pulses the emission intensity is already at 20% of initial value (Figure 4b), whereas the absorption band remains almost unaffected. On the other hand, the emission PB kinetics saturates after a few hundred pulses, while absorption properties are still changing after more than 10000 pulses. Beside being slower, the absorption PB kinetics appears much more complex than the fluorescence PB kinetics. While the fluorescence decreases along a relatively simple stretched exponential kinetics, suggesting a single physical process, the absorption kinetics of Figure 4d suggests at least three different phases. It is possible to observe an initial step, which lasts around 50 pulses, where the absorption coefficient decreases quite steeply. Then there is a quite-complex intermediate phase (until 2000 pulses), after which the absorption coefficient decreases in an approximately linear way. Overall, it is not possible to observe a correlation between the PB of the emission and absorption properties extended to all the investigated PB dose range. In particular, considering that the decrease in fluorescence intensity is initially much more pronounced than the decrease in absorption, our data imply that the almost total fluorescence quenching shown in 4a and 4b is actually associated with a massive reduction of the fluorophore QY. A possible hypothesis to explain these results is that UV irradiation easily induces the isomerization of the chromophore into a non-fluorescent form, complete after just a few hundred pulses,

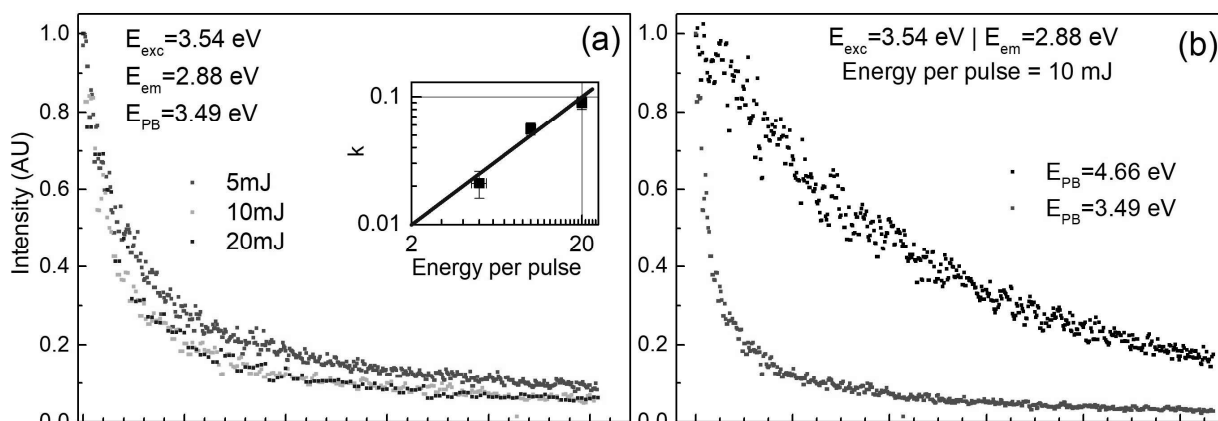


Figure 5: (a) PB Kinetics obtained at three different laser powers, plotted in terms of the energy administered by the laser. They clearly show that the PB kinetics are independent of irradiation power. (b) Log-Log graph of the process-efficiency parameter $k = 1/N_0$ as a function of the laser power. (c) Comparison between the PL PB kinetics obtained using a photon energy of 3.49 eV (red curve) and 4.66 eV (black curve).

but its absorption properties are not significantly affected. After the first few hundred pulses completely wipe out the emission, with only minor changes in the absorption, an almost complete disappearing of the absorption band occurs much later, after many thousands of pulses, suggesting a second stage in which UV irradiation induces the complete destruction of the chromophore responsible for the absorption transition.

In order to evaluate how the process is related to the power of the irradiation laser, the same experiment has been performed using different energies per pulse. The different kinetics we obtained by *in situ* PL measurements at different excitation intensities are shown in Figure S2, and display a clear increase of the photobleaching efficiency with laser power. However, if the same data are plotted in terms of given energy, rather than number of pulses (Figure 5a), they closely match each other. This agreement is a clear evidence of the linearity of the process, and implies that the absorption of a single photon from the high-intensity beam is sufficient (with a certain probability) to induce an irreversible photobleaching. This conclusion is further confirmed by two more evidences: (a) the linear relation, shown in the inset of figure 5a, observed between the efficiency parameter $k = \frac{1}{N_0}$ (where N_0 is the characteristic pulses number of the stretched exponential fit $y(N) = e^{-\left(\frac{N}{N_0}\right)^\beta}$ of the data in Figure S2) and the energy per pulse used during the process, and (b) the observation that a certain degree of photobleaching can be similarly induced by exposure of the sample to a simple lamp (Figure S3), provided the fluence on the sample is large enough. Therefore, the high peak intensity of the laser beam is not a necessary requirement for a photobleaching, which is another indication of a linear PB process.

While the PB process displays a clear intensity- dependence, we verified that it is almost independent of concentration (Figure S4). This result indicates that PB is a process occurring within one object at the time, rather than involving a fluorophore-fluorophore interaction. Finally, we also did an additional targeted experiment changing the PB photon energy to 4.66 eV. In Figure 5b, the results of this experiment are compared with those obtained with the standard PB photon energy of 3.49 eV, used in all the other experiments. The data indicate a highly increased efficiency of the PB process when the photon energy equals 3.49 eV. Considering that this value is close to the absorption peak of the sample, this result suggests that the process could be in resonance with the main optical transition of the chromophore.

In general, irreversible changes of optically-active materials in solution or solid phase are often due to complex sequences of photochemical events triggered by multi-photon absorption [29, 30]. Despite the detailed photochemical process responsible for CD photobleaching cannot be fully elucidated here, our data point to a quite simple scenario, in which the first electronically excited state of the fluorescent chromophore has a certain probability of evolving irreversibly into a non-fluorescent form, causing the permanent deactivation of the emission of CDs within a few hundreds of UV pulses. This process is the one posing the main limitation to the photostability of these CDs under UV light. Only after several thousand of pulses, the surface chromophore is eliminated altogether, as we infer from *in situ* absorption experiments. As proposed before [34], this second stage

(5000-10000 pulses) is likely due to a carbonization of the chromophore, as suggested by the resemblance of the final absorption spectrum (Figure 1a) with the unstructured (π plasmon-like) absorption of carbonaceous cores [4, 48]. However, full carbonization is obviously not necessary for an irreversible fluorescence photobleaching to take place, considering that the emission is fully deactivated well before this stage (<500 pulses). Besides, some previous studies have proposed amorphous core CDs to be more sensitive to PB than crystalline core CDs [35, 37, 38]. Our results seem to contrast with this view: in fact, the most efficient phase of the PB process appears to involve only the direct interaction between the UV beam and the surface molecular chromophore, with no participation of the core structure, as also confirmed by the absence of any changes in the core-related absorption tail, even after very large irradiation doses.

Conclusions

We used optical absorption and fluorescence methods to study *in-situ* the photobleaching dynamics of citric acid and urea-derived carbon dots exposed to high intensity UV laser pulses. Our technique allows to reconstruct in detail the kinetics of the undergoing PB process, as a function of several relevant parameters, revealing a variety of information on the PB dynamics. The results indicate that the fluorescence photobleaching of CDs proceeds through two distinct phases: a first step involves the efficient conversion of surface chromophores into a non-fluorescent form, triggered by linear absorption at the peak of their near-UV absorption band. In this phase, only the emission efficiency is strongly reduced, with negligible changes of the absorption spectra. At higher fluences, a second phase begins in which we observe a stronger and irreversible change in the absorption spectrum, related to the complete and irreversible destruction of the molecular chromophores by UV irradiation. Additionally, the striking difference between the PB kinetics recorded in uniform and non-uniform illumination geometries provides direct evidence that the blue-emitting chromophores of these CDs are small molecular units. Part of these molecules are freely diffusing in solution, in a dynamical equilibrium with those adsorbed on CD surfaces. Finally, a detailed analysis of the PB kinetics reveals several more details on the photophysics of the system, previously unknown, such as the influence of disorder effects on the PB efficiency and a photoselection effect within the initial population of CDs.

Conflicts of interest

There are no conflicts to declare.

Acknowledgements

We thank the members of the LaBAM group for support and scientific discussions. We thank Dr. R. Messina (CNRS, France) for assistance in the preparation of the manuscript.

Notes and references

- 1 X. Xu, R. Ray, Y. Gu, H. J. Ploehn, L. Gearheart, K. Raker and W. A. Scrivens, *Journal of the American Chemical Society*, 2004, **126**, 12736.
- 2 A. Sciortino, A. Cannizzo and F. Messina, *C*, 2018, **4**, 67.
- 3 M. Semeniuk, Z. Yi, V. Poursorkhabi, J. Tjong, S. Jaffer, Z. Lu, and M. Sain, *ACS Nano*, 2019, **13**, 6224–6255.
- 4 Y. P. Sun, B. Zhou, Y. Lin, W. Wang, K. A. S. Fernando, P. Pathak, M. J. Mezziani, B. A. Harruff, X. Wang, H. Wang, P. G. Luo, H. Yang, M. E. Kose, B. Chen and L. M. Veca, *Journal of the American Chemical Society*, 2006, **128**, 7756.
- 5 F. Messina, L. Sciortino, R. Popescu, A. M. Venezia, A. Sciortino, G. Buscarino, S. Agnello, R. Schneider, D. Gerthsen, M. Cannas and F. M. Gelardi, *Journal of Materials Chemistry C*, 2016, **4**, 2598.
- 6 L. Cao, X. Wang, M. J. Mezziani, F. Lu, H. Wang, P. G. Luo, Y. Lin, B. A. Harruff, L. M. Veca, D. Murray, S. Xie and Y. Sun, *Journal of the American Chemical Society*, 2007, **129**, 11318.
- 7 M. T. Hasan, R. Gonzalez-Rodriguez, C. Ryan, J. L. Coffey and A. V. Naumov, *ACS Appl. Mater. Interfaces* 2019, **11**, 39035.
- 8 X. Li, L. Yan, J. Si, H. Xu and Yanmin Xu, *RSC Adv.*, 2019, **9**, 12732
- 9 M. Sun, C. Liang, Z. Tian, E. V. Ushakova, D. Li, G. Xing, S. Qu and A. L. Rogach, *J. Phys. Chem. Lett.*, 2019, **10**, 3094.
- 10 A. Sciortino, N. Mauro, G. Buscarino, L. Sciortino, R. Popescu, R. Schneider, G. Giammona, D. Gerthsen, M. Cannas and F. Messina, *Chem. Mater.* 2018, **30**, 1695.
- 11 S. Mondal, A. Yucknovsky, K. Akulov, N. Ghorai, T. Schwartz, H. N. Ghosh and N. Amdursky, *J. Am. Chem. Soc.*, 2019, **141**, 15413.
- 12 Y. Song, W. Shi, W. Chen, X. Li and H. Ma, *J. Mater. Chem.*, 2012, **22**, 12568.
- 13 D. Qu, M. Zheng, P. Du, Y. Zhou, L. Zhang, D. Li, Z. Zhao H. Tan, Z. Xie and Z. Sun, *Nanoscale*, 2013, **5**, 12272.
- 14 R. Liu, H. Li, W. Kong, J. Liu, Y. Liu, C. Tong, X. Zhang and Z. Kang, *Materials Research Bulletin*, 2013, **48**, 2529.
- 15 F. Zahir, S. J. Rizwi, S. K. Haq and R. H. Khan, 2005, **20**, 351.
- 16 A. Zhu, Q. Qu, X. Shao, B. Kong and Y. Tian, *Angewandte Chemie International Edition*, 2012, **51**, 7185.
- 17 W. F. Zhang, L. M. Jin, S. F. Yu, H. Zhu, S. S. Pan, Y. H. Zhao and H. Y. Yang, *J. Mater. Chem. C*, 2014, **2**, 1525.
- 18 M. J. Krysmann, A. Kelarakis, P. Dallas and E. P. Giannelis, *Journal of the American Chemical Society*, 2012, **134**, 747.
- 19 J. Schneider, C. J. Reckmeier, Y. Xiong, M. von Seckendorff, A. S. Susha, P. Kasak and A. L. Rogach, *J. Phys. Chem. C*, 2017, **121**, 2014.
- 20 Y. Song, Y. Zhu, S. Zhang, S. Fu, Y. Yang, L. Zhao and X. Yang, *J. Mater. Chem. C*, 2015, **3**, 5976.
- 21 Y. Xiong, J. Schneider, E. V. Ushakova and A. L. Rogach, *Nano Today*, 2018, **23**, 124.
- 22 R. Ludmerczki, S. Mura, C. M. Carbonaro, I. M. Mandity, M. Carraro, N. Senes, S. Garroni, G. Granozzi, L. Calvillo, S. Marras, L. Malfatti and P. Innocenzi, *Chem. Eur. J.* 2019, **25**, 11963.
- 23 J. B. Essner, J. A. KistLuis, L. Polo-Parada and G. A. Baker, *Chem. Mater.*, 2018, **30**, 1878.
- 24 F. Du, M. Zhang, X. Li, J. Li, X. Jiang, Z. Li, Y. Hua, G. Shao, J. Jin, Q. Shao, M. Zhou and A. Gong, *Nanotechnology*, 2014, **25**, 315702.
- 25 Q.-L. Zhao, Z.-L. Zhang, B.-H. Huang, J. Peng, M. Zhang and D.-W. Pang, *Chem. Commun.*, 2008, **41**, 5116.
- 26 S. Sahu, B. Behera, T. K. Maiti and S. Mohapatra, *Chem. Commun.*, 2012, **48**, 8835.
- 27 H. Li, X. He, Z. Kang, H. Huang, Y. Liu, J. Liu, S. Lian, C. H. A. Tsang, X. Yang and S. T. Lee, *Angewandte Chemie International Edition*, 2010, **49**, 4430.
- 28 N. C. Shaner, P. A. Steinbach and R. Y. Tsien, *Nature Methods*, 2005, **2**, 12.
- 29 L. Song, E. J. Hennink, T. Young and H. J. Tanke, *Biophysical Journal*, 1995, **68**, 2588.
- 30 T. Hirschfeld, 1976, **15**, 12.
- 31 H. C. Ishikawa-Ankerhold, R. Ankerhold and G. P. C. Drummen, *Molecules*, 2012, **17**, 4047.
- 32 H. Peng and J. Travas-Sejdic, *Chemistry of Materials*, 2009, **21**, 5563.
- 33 G. He, M. Shu, Z. Yang, D. Huang, Y. Ma, S. Xu, Y. Wang, N. Hu, Y. Zhang and L. Xu, *Applied Surface Science*, 2017, **422**, 257.
- 34 W. Wang, B. Wang, H. Embrechts, C. Damm, A. Cadranell, V. Strauss, M. Distaso, V. Hinterberger, D. M. Guldi and W. Peukert, *RSC Adv.*, 2017, **7**, 24771.
- 35 M. L. Liu, L. Yang, R. S. Li, B. B. Chen, H. Liu and C. Z. Huang, *Green Chem.*, 2017, **19**, 3611.
- 36 S. K. Das, Y. Liu, S. Yeom, D. Y. Kim and C. I. Richards, *Nano Lett.*, 2014, **14**, 620.
- 37 S. Zhu, Q. Meng, L. Wang, J. Zhang, Y. Song, H. Jin, K. Zhang, H. Sun, H. Wang and B. Yang, *Angew. Chem.*, 2013, **125**, 4045.
- 38 W. Wang, C. Damm, J. Walter, T. J. Nacken and W. Peukert, *Phys. Chem. Chem. Phys.*, 2016, **18**, 466.
- 39 Y. Xiong, J. Schneider, C. J. Reckmeier, H. Huang, P. Kasák and Andrey L. Rogach, *Nanoscale*, 2017, **9**, 11730.
- 40 L. Sciortino, A. Sciortino, R. Popescu, R. Schneider, D. Gerthsen, S. Agnello, M. Cannas and F. Messina, *J. Phys. Chem. C*, 2018, **122**, 19897.
- 41 Z. Yang, M. Xu, Y. Liu, F. He, F. Gao, Y. Su, H. Wei and Y. Zhang, *Nanoscale*, 2014, **6**, 1890.
- 42 L. Shi, J. Hai Yang, H. B. Zeng, Y. M. Chen, S. C. Yang, C. Wu, H. Zeng, O. Yoshihito and Q. Zhang, *Nanoscale*, 2016, **8**, 14374.
- 43 A. Sharma, T. Gadly, S. Neogy, S. K. Ghosh and M. J. Kumbhakar, *J. Phys. Chem. Lett.*, 2017, **8**, 1044.
- 44 Y. Gude, A. Das, T. Chatterjee and P. K. Mandal, *Phys. Chem. Chem. Phys.*, 2016, **18**, 28274.
- 45 M. Righetto, A. Privitera, I. Fortunati, D. Mosconi, M. Zerbetto, M. L. Curri, M. Corricelli, A. Moretto, S. Agnoli, L. Franco, R. Bozio and C. J. Ferrante, *Phys. Chem. Lett.*, 2017, **8**, 2236.
- 46 F. Ehrat, S. Bhattacharyya, J. Schneider, A. Löf, R. Wyrwich, A. L. Rogach, J. K. Stolarczyk, A. S. Urban and J. Feldmann, *Nano Letters* 2017, **17**, 7710.
- 47 S. Mura, L. Stagi, L. Malfatti, C. M. Carbonaro, R. Ludmerczki and P. Innocenzi, *J. Phys. Chem. A*, 2020, **124**, 197.
- 48 W. Liang, L. Ge, H. Hou, X. Ren, L. Yang, C. E. Bunker, C. M. Overton, P. Wang, Y.-P. Sun, *C* 2019, **5**, 70.
- 49 A. Sciortino, M. Gazzetto, G. Buscarino, R. Popescu, R. Schneider, G. Giammona, D. Gerthsen, E. J. Rohwer, N. Mauro, T. Feurer, A. Cannizzo, F. Messina, *Nanoscale* 2018, **10**, 15317.